

# The combined effect of transport and temperature on distribution and growth of larvae and pelagic juveniles of Arcto-Norwegian cod

Frode Vikebø, Svein Sundby, Bjørn Ådlandsvik,  
and Øyvind Fiksen

Vikebø, F., Sundby, S., Ådlandsvik, B., and Fiksen, Ø. 2005. The combined effect of transport and temperature on distribution and growth of larvae and pelagic juveniles of Arcto-Norwegian cod. — ICES Journal of Marine Science, 62: 1375–1386.

Temperature has been identified in field studies as the physical parameter most influential on growth and recruitment of Arcto-Norwegian cod. However, it has been pointed out by many authors that temperature in this context has not only direct effects on the cod, but also indirect effects through lower trophic levels. Moreover, it has been said that temperature might also be a proxy for other climatic parameters. The present paper analyses the direct quantitative effects of temperature on larval and pelagic juvenile growth from spawning in Lofoten until the 0-group fish settle in the Barents Sea. The approach taken is that of a modelling study, supported by analysis of existing data on fish stocks and climate. It is shown that transport and temperature alone can reproduce key features of the 0-group weight distribution and concentration in the Barents Sea for two consecutive years. The extent of the dispersion of the larvae and pelagic juveniles, as well as the ambient temperature they experience on their route, are shown to depend upon their depth in the water column and, to a lesser degree, the time of spawning.

© 2005 International Council for the Exploration of the Sea. Published by Elsevier Ltd. All rights reserved.

Keywords: Arcto-Norwegian cod, growth, larvae and pelagic juveniles, ocean model, transport.

Received 30 January 2005; accepted 20 May 2005.

F. Vikebø, S. Sundby, and B. Ådlandsvik: *Institute of Marine Research, PO Box 1870 Nordnes, N-5817 Bergen, Norway.* Ø. Fiksen: *Department of Biology, University of Bergen, PO Box 7800, N-5020 Bergen, Norway.* Correspondence to F. Vikebø: tel: +47 55238441; fax: +47 55238687; e-mail: [frode.vikebo@imr.no](mailto:frode.vikebo@imr.no).

## Introduction

The spawning grounds of the Arcto-Norwegian cod (ANC) are located along the coast of middle and northern Norway (Figure 1a), particularly in the Lofoten and Vesterålen area, where up to 70% of the spawning occurred between 1983 and 1985 (Sundby and Bratland, 1987). Compared with other Atlantic cod (*Gadus morhua* L.) stocks, there is a long route of pelagic-free drift for the offspring from spawning in March until early May along the coast, until the juveniles settle to the bottom in the Barents Sea in September to October. During this critical period, with respect to the formation of year-class strength, the eggs, larvae, and pelagic juveniles drift from between 600 to 1200 km.

Eggs, larvae, and pelagic juveniles are carried north-eastwards by the Norwegian Coastal Current (NwCC, Figure 1a). Lateral spreading takes part of the population into the Norwegian Atlantic Current (NwAC), which flows

parallel to the NwCC and is warmer than the NwCC at the time of spawning. Five months after spawning, they are surveyed pelagically by the international 0-group survey and are found spread over the entire area occupied by Atlantic Waters in the Barents Sea (ICES, 1985, 1986). At that time of the season, the NwCC has become the warmer water mass of the two. After this stage, they settle to the bottom. Abundance indices of ANC at the early juvenile stage (2–3 months), 0-group stage (4–5 months), and for three-year-old fish are estimated based on trawl surveys and virtual population analysis. Correlation analysis indicates high correlation of both the early juvenile stage and 0-group stage with the three-year-old fish (Sundby *et al.*, 1989). Ottersen and Loeng (2000) show that there is a close link between abundance and length of cod at the 0-group stage and between length at the 0-group stage and the year-class strength of the three-year-old fish. Hence, the year classes of cod are generally determined

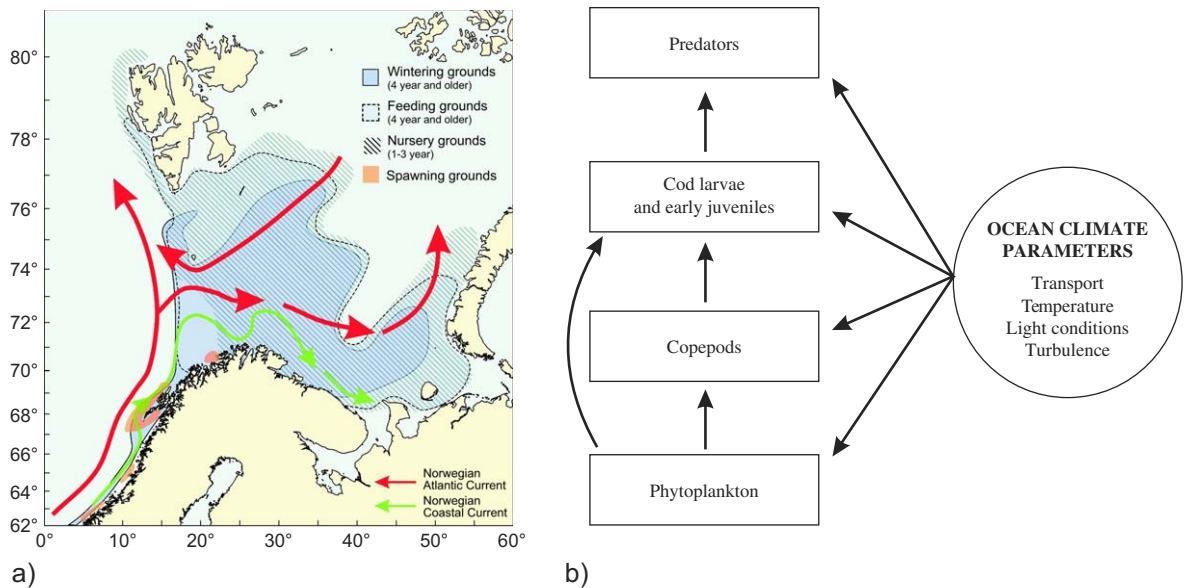


Figure 1. Spawning and nursery grounds of the ANC in relation to the Norwegian Atlantic Current and the Norwegian Coastal Current (a). Influence of ocean climate parameters in trophic transfer (b) (from Sundby, 2000).

during the drift phase from the spawning grounds to the nursery grounds.

During the last decade or so, several studies have shown that numerical models are suitable tools in the study of transport of fish larvae. This includes modelling studies concerning gadids on Georges Bank (Werner *et al.*, 1993; Lough *et al.*, 1994), in the North Sea (Heath and Gallego, 1998; Gallego *et al.*, 1999), and in the Baltic (Voss *et al.*, 1999; Hinrichsen *et al.*, 2002, 2003). These studies have contributed to the development from simple particle drift to individual-based models (IBM) including dependency on biotic and abiotic parameters (Werner *et al.*, 2001). For the ANC, an earlier attempt to model the transport of larvae and pelagic juveniles from the spawning grounds in Lofoten to the nursery ground in the Barents Sea was partly successful (Ådlandsvik and Sundby, 1994). They concluded that their model failed to resolve key features along the continental shelf because of insufficient horizontal resolution, although the interannual variability in the location of the concentrations of 0-group cod seemed to be quite consistent with field data from surveys. However, none of the previous modelling studies of the ANC included the growth of larvae and pelagic juveniles.

Individual growth of cod larvae and juveniles shows functional relationships to biotic and abiotic parameters (Figure 1b). The biotic parameter of importance for growth is food availability. Abiotic parameters of importance are ocean climate parameters such as advection, temperature, turbulence, and light conditions, the last-named varying with cloud conditions and latitude. One of the most important effects is felt through the influence of temperature on feeding intensity, metabolic rates, and thereby growth

(Otterlei *et al.*, 1999). Moreover, light conditions and wind-induced turbulence are other important abiotic parameters in relation to behavioural responses affecting growth of fish (Sundby and Fossum, 1990; Suthers and Sundby, 1996; Fiksen *et al.*, 1998). Indirect effects of temperature, through lower trophic level interactions, are similarly important, particularly the production at lower trophic levels. The copepod *Calanus finmarchicus* is the dominant mesozooplankton in the Subarctic Gyre of the northern North Atlantic and the main prey item for the ANC larvae and juveniles. It is adapted to the spring bloom of the region with feeding and reproduction during spring and summer, and hibernation at depth during winter. Through advection by the NwAC, the *C. finmarchicus* production spills over from the core regions onto the adjacent shelves, e.g. the shelf off Norway and the Barents Sea. Therefore, Sundby (2000) suggested that the recruitment–temperature relation for the Atlantic cod is a proxy for the food abundance during the early stages, explained by the advection of warm *C. finmarchicus*-rich waters from the core production regions to the habitat of cod.

Only small year classes are produced when temperatures in the early larval distribution areas are low, while year classes of all strengths are produced under higher temperatures (Ottersen and Loeng, 2000). This implies that high temperatures are a necessary, although not a sufficient, condition for the formation of strong year classes. Ellertsen *et al.* (1989) relate this to the delay in spawning of *C. finmarchicus* during cold years, and the subsequent mismatch with the spawning of ANC. However, there is less chance for the formation of a strong year class unless there is a high spawning-stock biomass (Ottersen and Sundby,

1995). Generally, pelagic juveniles are smaller in the north-eastern region of the nursery grounds than those closer to the spawning grounds farther to the southwest (Bjørke and Sundby, 1987; Suthers and Sundby, 1993). In fact, juvenile size is proportional to the degree-days (integrated temperature along the drift route) after hatching (Suthers and Sundby, 1993). However, these distribution patterns might also be influenced by indirect effects such as food abundance (Sundby, 2000). Increased understanding of how temperature influences the recruitment of ANC under present climate conditions is a prerequisite for studying the effect of possible climate changes on the cod stock in the future.

The purpose of this study is to investigate the direct effects of transport and temperature on distribution and growth of ANC. In order to do so, we used a circulation model combined with an individual-based larval and juvenile model. The models simulate transport of larvae and pelagic juveniles for two subsequent years, while keeping a record of the individual temperature histories, permitting calculation of temperature-dependent growth, from spawning until settlement at the nursery grounds. The years 1985 and 1986 were chosen for the modelling exercise because of their differences both in distribution and individual weight of the 0-group cod (Figure 2). Also, the total abundance of 0-group cod was higher in 1985 than in 1986, and the centre of biomass was farther to the west. The distribution in 1985 covered a larger area than in 1986, and the average length of 0-group cod, and therefore the weight (Ellertsen *et al.*, 1989), was significantly lower in 1986 than in 1985 (Ottersen and Loeng, 2000). By doing this, we wish to answer the following questions. Will the model be able to reproduce observed 0-group distributions? In what way will vertical distribution of larvae and pelagic juveniles affect 0-group distribution and weight? Will the

time of spawning affect growth and distribution of 0-group cod?

## The model system

The circulation model used in this study is the Regional Ocean Modelling System (ROMS), version 2.0 (Shchepetkin and McWilliams, 2005), <http://marine.rutgers.edu/po/models/roms/>. This is a free-surface, hydrostatic, primitive equation ocean model that uses stretched terrain-following coordinates in the vertical and orthogonal curvilinear coordinates in the horizontal. The model solves the primitive equations by the finite differences method on an Arakawa C-grid. Mode splitting between the external barotropic mode and the internal barotropic mode is applied. A third-order accurate predictor (Leap-frog) and corrector (Adams–Molton) algorithm is used for the time-stepping. The level 2.5 Mellor–Yamada turbulence closure scheme (Mellor and Yamada, 1982) is also used.

Monthly mean climatological values of velocity, temperature, salinity, and water elevation in addition to four dominant tidal constituents ( $M_2$ ,  $S_2$ ,  $K_1$ , and  $N_2$ ) are used to specify the lateral boundary conditions. The model forcing also includes daily NCEP/NCAR reanalysed windstress, air pressure, and ocean–atmosphere heat exchange for the years 1985 and 1986 (Kalnay *et al.*, 1996). The short-wave radiation is multiplied by a factor, which decreases linearly from 1 at the southernmost boundary to 0.5 at the northernmost boundary, in order to reproduce measured temperature distributions. The rationale behind this is that the NCEP/NCAR cloud cover for the Barents Sea seems to be too low (Budgell, 2005). Additional forcing is given by prescribed river run-off from 12 freshwater sources along the coast. The initial description of water elevation,

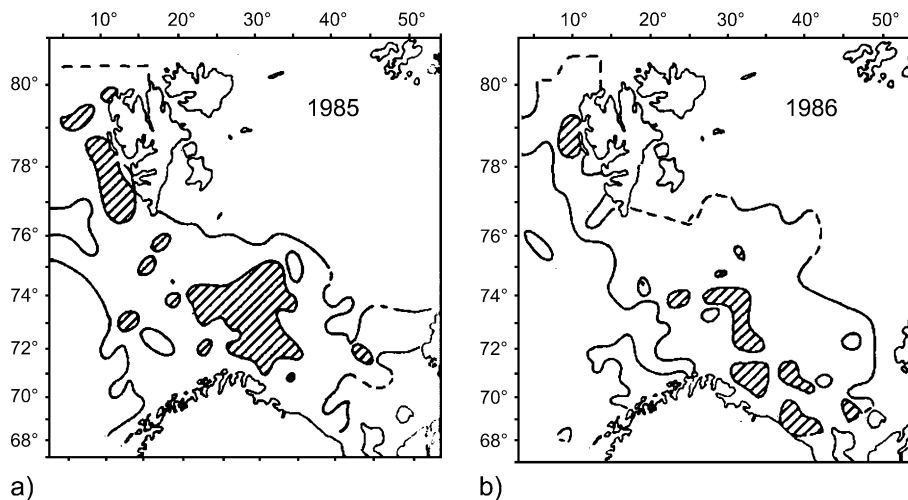


Figure 2. Distribution of 0-group cod for 1985 (a) and 1986 (b). The outer isoline indicates one fish per nautical mile of tow, whereas the hatched area indicates more than 85 fish per nautical mile of tow (ICES, 1985, 1986).

velocity, temperature, and salinity is taken from the 20-km DNMI-IMR diagnostic climatology (Engedahl *et al.*, 1998), so no interannual variations are imposed through the lateral boundaries. Relaxation towards climatology at the lateral boundaries is done with a flow relaxation scheme (FRS; Martinsen and Engedahl, 1987) for the baroclinic variables including tracers (Ådlandsvik and Budgell, 2003) and a combination of Chapman and Flather conditions for the free surface and the barotropic variables (Flather, 1976; Chapman, 1985). Flow relaxation is performed throughout the water column at the ten outermost cells adjacent to the boundary. The model grid consists of  $148 \times 318$  cells (Figure 3) with 25 vertical sigma-layers. The resolution increases from about 3.8 km in the southernmost parts, 5.3 km in the Vestfjord, and up to 8.5 km in the northernmost parts of the model domain. The bottom topography is taken from Etopo2, which gives a horizontal resolution of about 3.5 km.

A general evaluation of the model shows that it reproduces the observed hydrography and current metre measurements at stations and sections (Vikebø, 2005). More specifically, it reproduces the seasonal variation of temperature throughout the water column at the spawning ground in the Vestfjord, the observed vertical distribution of temperature at the Gimsøy section off western Norway, and the Fugløy section at the western entrance to the Barents Sea, as well as the volume flux trough in the Fugløy section (Figure 3).

An individual-based model is implemented into the larval and pelagic juvenile drift module to simulate how growth is influenced by changes in the ocean climate. This model simulates individual growth of larvae and pelagic juveniles from the functional relationships to biotic and abiotic parameters, e.g. Fiksen *et al.* (1998). Particles are released as a patch at a well-known spawning site inside the Vestfjord (Figure 3), covering about  $15 \times 15$  km, equally distributed at 10-, 20-, and 30-m depth. The input

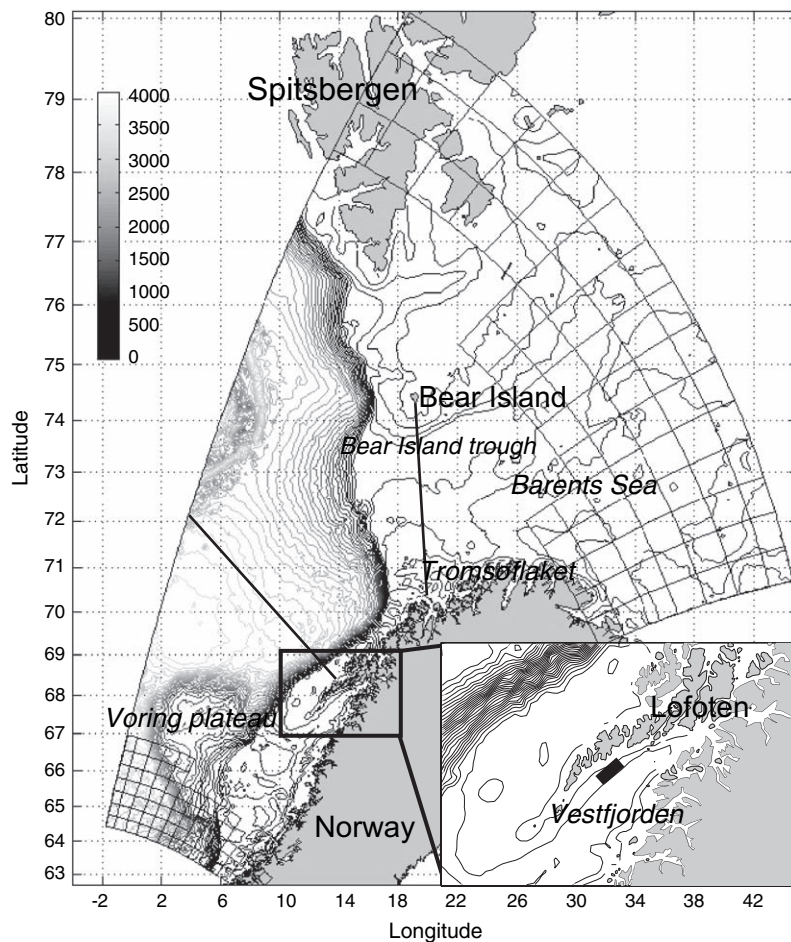


Figure 3. The model area with depth contours at every 100 m and part of the grid showing every ten grid-cell. Particles are released in the Vestfjord covering a fixed area indicated by the black box. The solid lines represent standard sections: the Gimsøy Section off western Norway and the Fugløy Section at the western entrance to the Barents Sea.

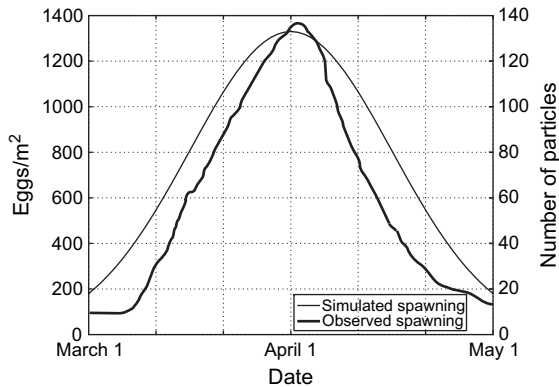


Figure 4. Averaged observed spawning intensity of cod (eggs  $m^{-2}$ ) in Lofoten for the years 1976 to 1983 as presented in Ellertsen *et al.* (1989) (solid line) and simulated spawning intensity (dashed line).

of particles has a Gaussian distribution in time in order to simulate observed spawning intensity (Figure 4).

Particles are moved forward by the updated velocity fields from the hydrodynamic model. Earlier work had included a random walk in addition to advection in order to parameterize Fickian diffusion (Csanady, 1973; Ådlandsvik and Sundby, 1994). The diffusion coefficient,  $K$ , could be tuned in order to increase the correspondence between simulations and observations. There is no added random walk to the velocity field transporting particles in this study, which may cause an underestimation of the spread of particles. However, with decreasing grid size, the need for artificial diffusion is reduced, as the range of resolved eddies and velocity shear is increased, leading to greater spreading of the particles.

The ambient temperature history of each particle is recorded as it moves. Growth of each larva and pelagic juvenile can then be estimated by combining the temperature-dependent growth functions presented in Otterlei *et al.* (1999) and Björnasson and Steinarsson (2002). In both these laboratory studies, cod were reared in tanks at fixed temperatures with unlimited food. Otterlei *et al.* (1999) reared larvae for eight weeks at fixed temperatures

ranging from 4 to 14°C, with steps of 2°C, and initial weight of 0.030 mg (dry weight). A Gompertz function was fitted to the data:

$$\ln DW(t) = \ln DW_0 - A + A \left[ \frac{\ln DW_{inf} - \ln DW_0 + A}{A} \right]^{(1 - e^{-(a+bT)t})}, \quad (1)$$

where  $DW_0$  is the initial weight of the larvae,  $DW_{inf}$  indicates the range of the data set used to fit the function, and  $T$  is the temperature (Figure 5a). The parameter values were  $DW_0 = 0.030$  mg,  $DW_{inf} = 250$  mg,  $A = 0.198$ ,  $a = 0.0061$ , and  $b = 0.0044$ . Björnasson and Steinarsson (2002) reared larvae for several years and came up with a functional relationship for the size range 2–5000 g (wet weight) for temperatures ranging from 2 to 16°C, with irregular steps of between 2 and 3°C. Specific growth rate was presented as per cent per day:

$$G = aW^{(b+cT)}, \quad (2)$$

where  $W$  is the wet weight,  $T$  the temperature, and  $a$ ,  $b$ , and  $c$  are constants with the following values:  $a = 0.5735$ ,  $b = -0.1934$ , and  $c = -0.02001$  (Figure 5b). The smallest initial weight of larvae in the study was about 1 g and, therefore, the model does not apply to cod larvae <1 g. As we wish to estimate the temperature-dependent growth of larvae and pelagic juveniles from newly hatched to 0-group stage (4–5 months), we combined the two temperature–growth functions. The ratio of dry weight to wet weight is size dependent, but, at the interface between the two models, it is about 1:5. Figure 6 shows the combined growth of cod during 200 days from an initial weight of 0.030 mg dry weight with the interface between the two models at three different weights: 100, 150, and 200 mg dry weight. These functional relationships between growth and temperature are based on fixed temperatures throughout the growth period, though this is obviously not the case for the particles in our simulations. Therefore, the subsequent

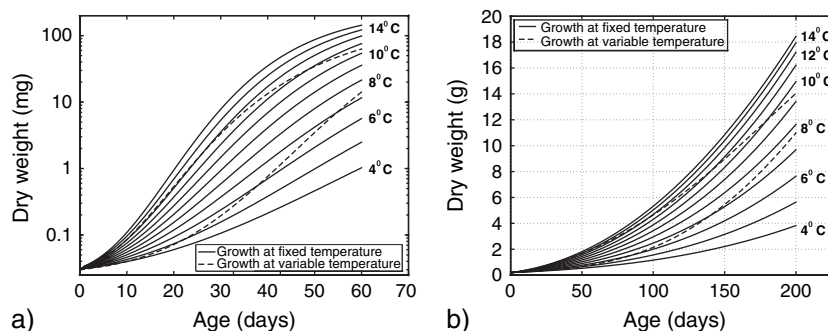


Figure 5. Temperature-dependent growth for Atlantic cod (*Gadus morhua*) with unlimited food availability at fixed temperatures as described by Otterlei *et al.* (1999) (a) and Björnasson and Steinarsson (2002) (b). The upper (lower) dotted line is the growth curve for a particle experiencing a linear increase (decrease) in temperature from 4 to 14°C (14 to 4°C).

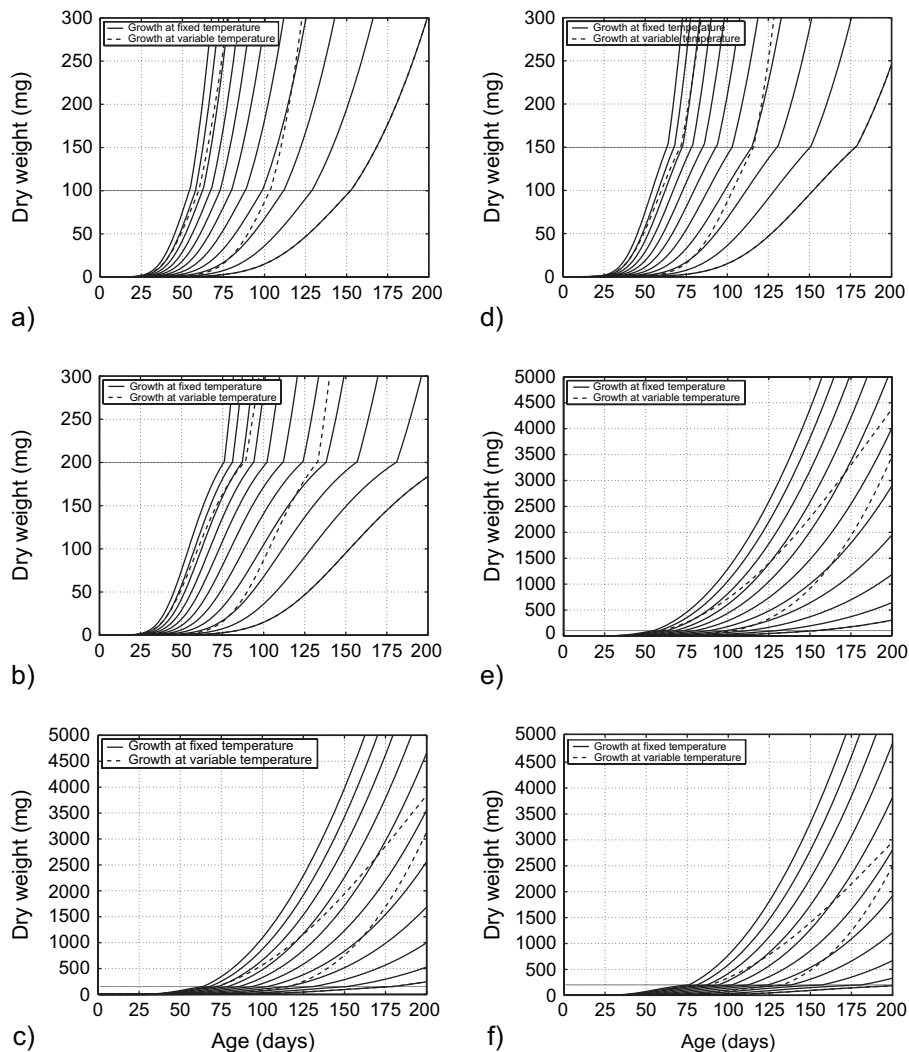


Figure 6. Combined temperature-dependent growth using Equations (1) and (2) in the text, with the interface at 100 (a, b), 150 (c, d), and 200 mg dry weight (e, f). The upper (lower) dotted line is the growth curve for a particle experiencing a linear increase (decrease) in temperature from 4 to 14°C (14 to 4°C).

daily growth is found as the difference between its current weight and its weight one day later, deduced from its last updated ambient temperature. When daily growth exceeds 100/150/200 mg dry weight, further daily temperature-dependent growth is calculated using Equation (2). It appears that the decrease in growth rate with size in the Otterlei-model may be too strong, as juveniles grow at higher rates in the Björnasson and Steinarsson model. Such effects could arise if the prey in the rearing experiment were too small for optimal growth of the largest larvae. Therefore, we chose to extrapolate the Björnasson and Steinarsson model down to 100 mg. Growth for a particle experiencing a linear increase in temperature from 4 to 14°C and a decrease from 14 to 4°C is shown on all Figures as dotted curves.

## Results and discussion

### Transport and growth of larvae and pelagic juveniles

Particles released at the spawning site inside the Vestfjord and transported by the circulation model result in 0-group distributions as shown in Figure 7. The colours indicate the individual simulated wet weights, based on the temperatures experienced along the route and the temperature-dependent growth relationships described in Equations (1) and (2). This figure and the ones that follow show distributions in late August, five months after peak spawning. Comparison of the simulated 0-group distributions with the observed distributions (Figure 2) reveals many of the same features. The centre of gravity for the 0-group

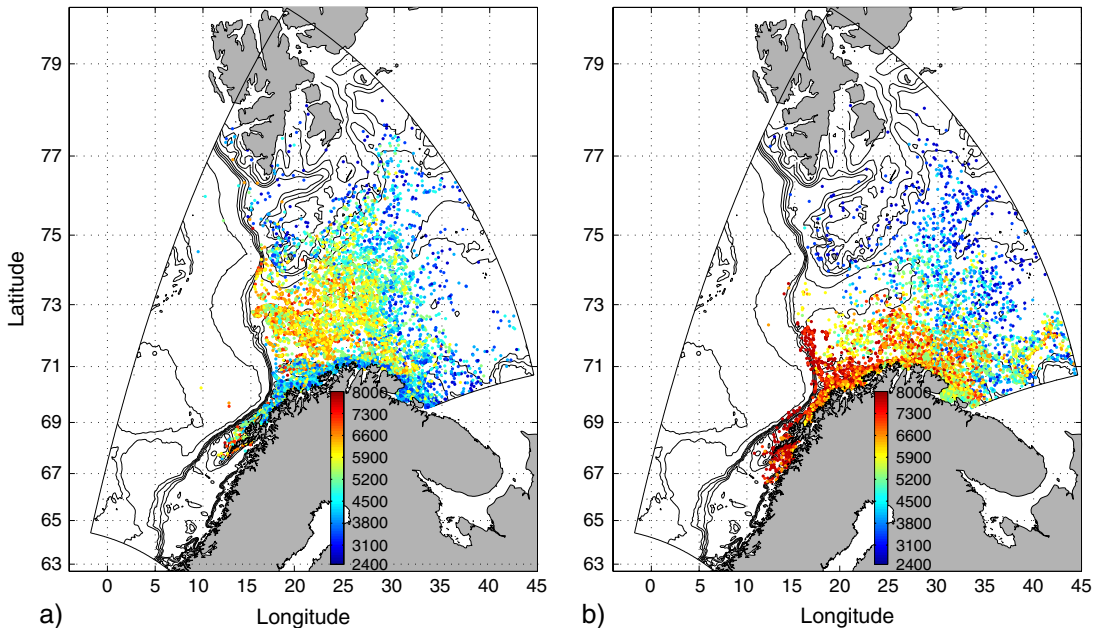


Figure 7. Simulated distribution of 0-group cod in late August, four to six months old depending on spawning, with atmospheric forcing from 1985 (a) and 1986 (b), and all particles released inside the Vestfjord, the main spawning site. The colour scale indicates wet weight in milligrams.

distribution in 1986 is more southeastern ( $71^{\circ}77'N$   $29^{\circ}61'E$ ) than in 1985 ( $72^{\circ}30'N$   $26^{\circ}07'E$ ). Both the simulated and the observed northernmost limits of the pelagic juveniles east of Spitsbergen (Figure 3) are around  $76^{\circ}N$ . Observed distributions stretch farther east than those simulated, probably because of the limited extent of the model domain in this direction. For 1986, many larvae are retained around the spawning ground in the simulation, resulting in a delayed advection towards the north. Many pelagic juveniles were distributed on the western side of Tromsøflaket, while few were found in the Bear Island trough, consistent with the observations. Also, it is clear from both simulations and observations how the fronts in the northeastern parts of the Barents Sea limit the distributions.

Simulated weight distributions show, in general, a higher weight of pelagic juveniles in the western Barents Sea than farther east, consistent with the observations presented in Suthers and Sundby (1993). Those authors discuss two hypotheses causing the observed distribution: differences in water temperature and food availability. Only temperatures were measured during the surveys where the data were collected, and they found a high correlation between growth and temperature. However, Sundby (2000) argues that temperature is a proxy for food abundance, since the core region of the *C. finmarchicus* has a higher temperature during the early juvenile stages than the adjacent shelves, i.e. the high correlation is due to advection of warm *C. finmarchicus*-rich water onto the shelf where the spawning and nursery grounds of cod are located.

The NwAC flows along the shelf edge, bifurcating north-west of the Tromsøflaket, with a branch entering the Barents Sea adjacent to the wedge-shaped NwCC close to the Norwegian coast, and the other branch following the shelf edge towards west Spitsbergen. Part of the NwAC flowing towards Spitsbergen enters the Barents Sea through the Bear Island trough ( $73^{\circ}N$   $18^{\circ}E$ , extending eastwards). Spawning in the Vestfjord occurs during March–May in the NwCC, which is colder than the NwAC and remains so until about June. Owing to horizontal mixing

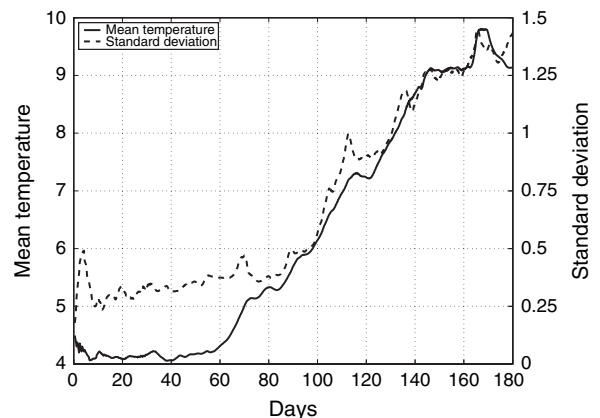


Figure 8. The simulated average and standard deviation of the ambient temperature for larvae and juveniles as a function of time since release at the spawning ground in the Vestfjord.

caused by wind and topographic effects, part of the larvae released in the NwCC will be displaced into the NwAC. Larvae transported northwards may therefore either be advected by the colder NwCC to the eastern parts of the Barents Sea, by the warmer NwAC to the central and western parts of the Barents Sea, or by the NwAC along the shelf edge to the west of Spitsbergen. The route greatly affects the degree-days and hence the growth.

The simulated average and standard deviations of the ambient temperature for larvae and pelagic juveniles as a function of time are shown in Figure 8. ANC spawning in the Vestfjord are located where the water temperatures range from about 4 to 6 °C, quite consistent with the simulated values. As the larvae and pelagic juveniles are transported from the spawning ground towards the nursery ground, both the average and standard deviation of ambient

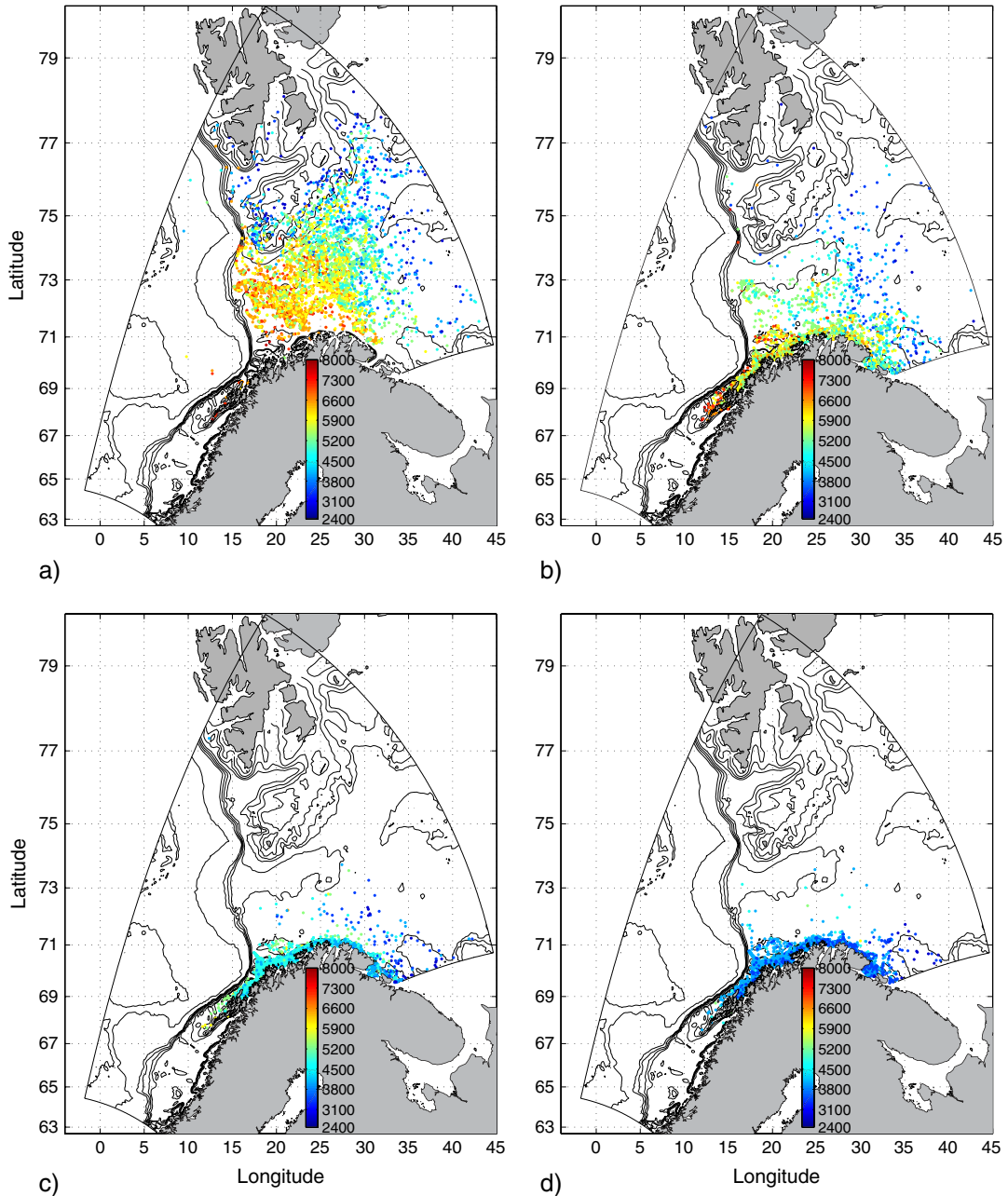


Figure 9. Juvenile distribution and weight (mg dry weight) in late August for larvae and juveniles held at 1 m (a), 10 m (b), 20 m (c), and 30 m (d).

temperature increase. Larvae trapped in the NwCC during the initial stages of the pelagic-free drift phase experience the lowest average ambient temperature. At the 0-group stage, juveniles that are advected farthest to the northeast in the Barents Sea enter Arctic Water, which limits their average ambient temperature. The stepwise increase in standard deviation of ambient temperatures reflects the horizontal variance of the distribution. The low-frequency change in the average and standard deviation of the ambient temperature, from a steady low level through an increase up to a higher level, is caused by the combined effect of seasonal warming and the advection of larvae and pelagic juveniles from the shelf area outside the spawning ground to the Barents Sea waters. Temporary retention above the Tromsøflaket, which concentrates larvae and pelagic juveniles through topographic effects, prolong the transport time towards the nursery grounds (Bjørke and Sundby, 1987). The superimposed high-frequency changes in the time-series are caused by variability in the atmospheric forcing.

#### Depth-dependent transport

Eggs are hatched and become larvae in about three weeks after they are spawned. This transition will affect their vertical distribution and hence their horizontal transport. The vertical distribution is also affected by winds (Sundby, 1983). During calm conditions, eggs were found in the entire upper mixed layer, with highest concentration at the surface and most eggs above 20 m. During windy conditions, eggs are mixed deeper in the water column. Increased winds will not only affect the vertical distribution, but also the amount of horizontal spreading. Larvae are also found in the upper mixed layer, with the majority distributed in the upper 30 m. Concentrations peak between 10 and 20 m, with a low concentration above 5 m (Ellertsen *et al.*, 1989). There is little evidence of diel migration of

larval and pelagic juvenile cod in this region, probably related to the 24-h daylight during summer. The egg stage is not included in this study, but the fact that, generally, eggs are distributed higher in the water column than larvae, means that an initial transport close to the surface is more representative than transport at greater depths.

Figure 9 shows the area-dependent weight distributions five months after peak spawning for the depths 1, 10, 20, and 30 m. Clearly the depth of larvae and pelagic juveniles has a great effect on both their horizontal concentrations and their area-dependent weight distributions. All the pelagic juveniles that were kept fixed at 1-m depth (Figure 9a) have left the spawning ground and are spread out in the entire Barents Sea, away from the coast. Most of them are limited by the continental shelf edge and the frontal areas to the north and east in the model domain. The 0-group distributions indicate higher weights in the western than in the eastern parts of the Barents Sea. At 10-m depth more pelagic juveniles are retained close to the spawning ground. The distribution is located closer to the coast, and farther away from the shelf edge and the frontal zones. Also at this depth, however, higher weights are found in the southwestern parts of the nursery ground. At 20- and 30-m depths, pelagic juveniles stay close to the coast as they are advected northwards. The larger ones are still found towards the southwest. Water temperature decreases with depth, and so does larval and pelagic juvenile growth. If a prescribed horizontal diffusion (random walk) was added independent of depth, it would still result in faster growth and more dispersion closer to the surface, but deeper in the water column, more larvae and pelagic juveniles would be transported away from the coast.

Figure 10a shows the average temperature for the larvae and pelagic juveniles for each depth as a function of days from initialization. The near-surface ones have the highest average temperature increase until peaking in late July, around day 150. It is clear that seasonal warming occurs

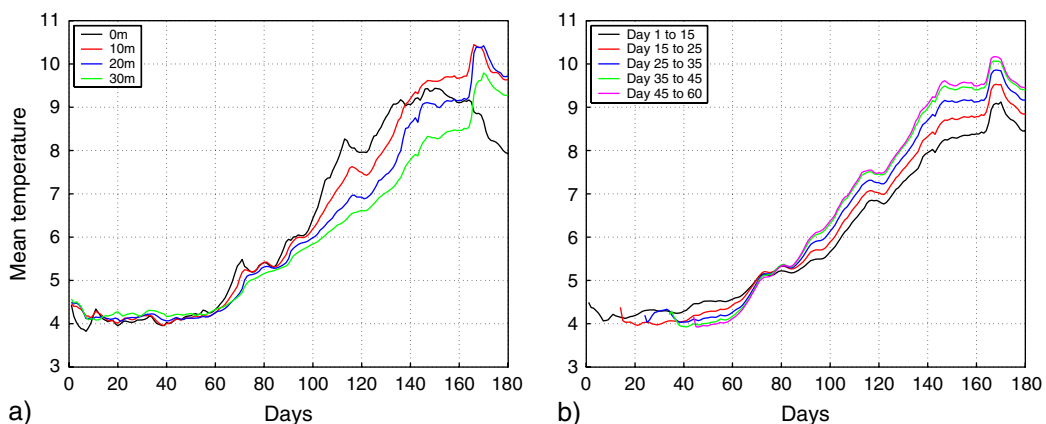


Figure 10. Average ambient temperature for particles held at 1-, 10-, 20-, and 30-m depth, during the time from the input of the first particles March 1 and 180 days forward (a). Average ambient temperature for particles starting at different times during the temporal Gaussian distributed hatching, days 1 to 15, 15 to 25, 25 to 35, 35 to 45, and 45 to 60 (b).

with a time-lag and decreasing amplitude down through the water column. Also, the peak is earlier for the near-surface larvae and pelagic juveniles because an increasing number of them reach the colder waters in the northern and eastern parts of the Barents Sea.

Larvae and pelagic juveniles in the near-surface habitat grow faster and are dispersed more widely in the Barents

Sea (Figure 9). If their prey were to be distributed deeper in the water column, cod would face a trade-off between being located where, on the one hand, there is more prey but slower temperature-dependent growth and less dispersal and, on the other, less prey but faster temperature-dependent growth and more dispersal. Quantifying this trade-off is important.

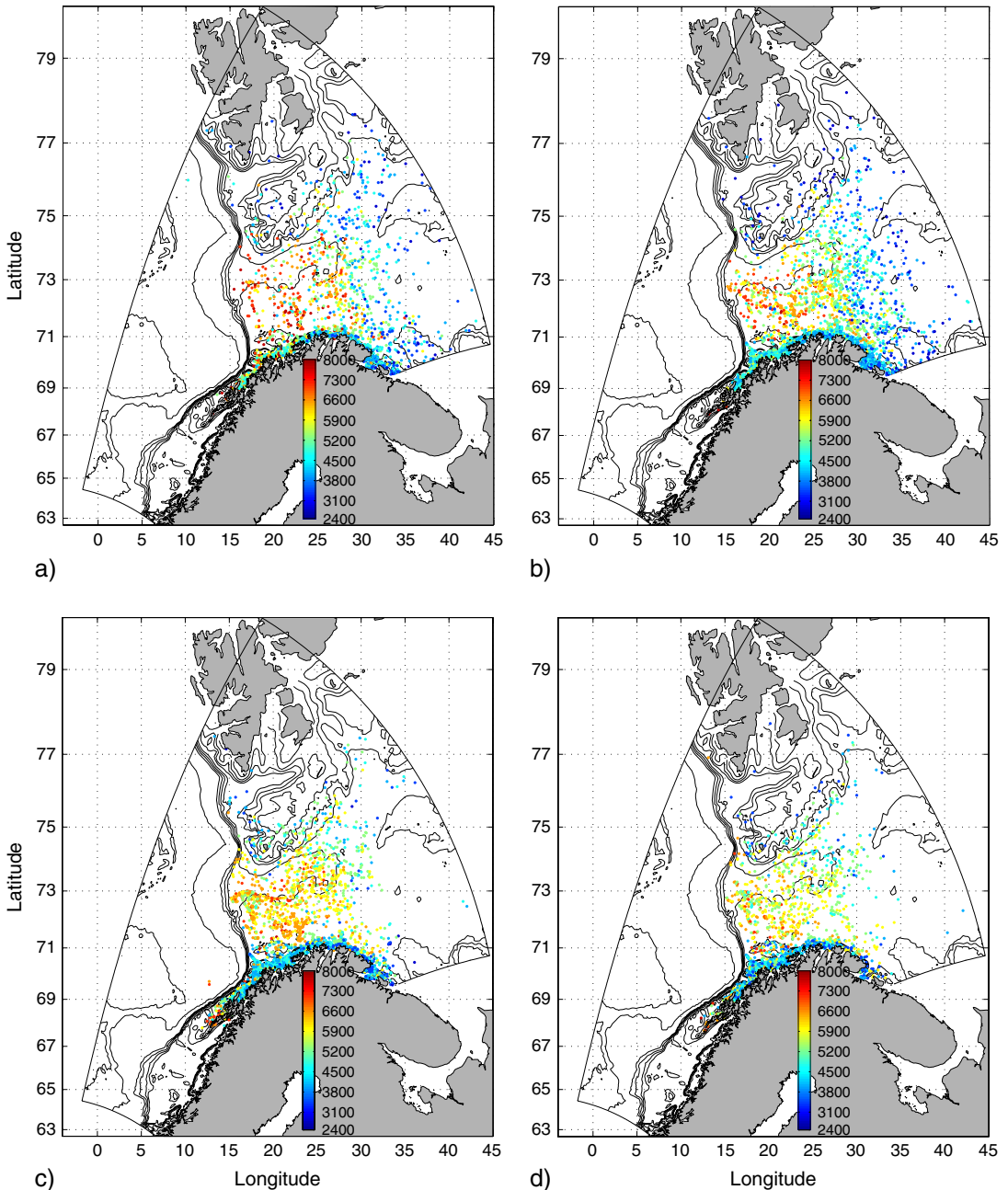


Figure 11. Juvenile distribution and weight (mg dry weight) in late August for larvae and juveniles released during days 1 to 15 (a), 15 to 25 (b), 35 to 45 (c), and 45 to 60 (d).

### Dependence on time of spawning

Distinguishing between larvae and pelagic juveniles that were released earlier and later during spring reveals differences in the 0-group distributions. Figure 11 shows 0-group distributions by late August for those initialized during days 1 to 15, 15 to 25, 35 to 45, and 45 to 60. All distributions cover a large part of the nursery ground in the Barents Sea, though the variance decreases with a later hatching time. Variance for the later releases is 74% of that for the earlier releases, with decreasing variance caused by decreasing winds towards summer and the reduced time of transport. All distributions show higher weights in the western than in the eastern parts of the Barents Sea. The weight range is higher for those released early, both because they are oldest, and because strong wind-induced initial horizontal spreading has enabled them to be advected far to the east, where the ambient temperature is low. Figure 10b shows the time-evolving averaged ambient temperature for groups of larvae and pelagic juveniles categorized by their time of initialization. The curves indicate that those released later get more quickly to higher average temperature than those released earlier because of seasonal warming. From day 70 onwards, the curves diverge, though they display the same characteristic shifts superimposed on the general trend. The reason for this divergence is that earlier releases stretch farther east into the Barents Sea where the temperature is lower. Large-scale windforcing is the reason for the superimposed shifts on the general trend.

### Concluding remarks

The simulations reproduce the observed key features of 0-group cod distributions for the years 1985 and 1986. (i) The simulated area-dependent weight distributions indicate larger larvae and pelagic juveniles in the western parts of the Barents Sea than farther east; (ii) the centre of gravity is more eastern in 1986 than in 1985; (iii) the distributions are limited to coastal and Atlantic Water masses; and (iv) prolonged transport time from the spawning ground to the nursery ground owing to retention above bank structures along the shelf. This indicates that transport and temperature-dependent larval and pelagic juvenile growth alone can reproduce key features of the 0-group weight distribution and concentration in the Barents Sea.

The vertical placement of larvae and pelagic juveniles has a significant impact on both the later horizontal distribution and weight. Larvae and pelagic juveniles drifting close to the surface are more likely to end up in the central or western Barents Sea, while those lower in the water column are more likely to end up close to the Norwegian coast or the eastern Barents Sea.

Earlier released larvae and pelagic juveniles have a higher mean and standard deviation of 0-group weights and are geographically more widespread as a consequence of longer transport time and stronger winds earlier in the

year. However, the temperatures experienced by both the individuals and the 0-group distributions by August are less dependent on the time of spawning than on the vertical placement of the larvae and pelagic juveniles. Food availability is not considered in the model in its present form. However, this might affect the dependence of the growth on time of spawning owing to the “match–mismatch” of prey and predators (Hjort, 1914).

The simulations reproduce the variations in horizontal concentration of these two years, though the differences in average weights are not. The year 1985 produced significantly higher average weight (and length) of 0-group cod than 1986 (Ottersen and Loeng, 2000). It is thought that the main reason this is not captured in the simulations is because the lateral boundary conditions are taken from climatology, and do not contain any interannual variations. Using interannual variations on these boundaries, in the same way as for the atmospheric forcing, is considered to be the most important factor to improve the model results. This would also enable us to estimate year-to-year variations in recruitment, since this is linked to the abundance of 0-group cod (Sundby *et al.*, 1989) and their condition (Ottersen and Loeng, 2000). This is one of the topics we plan to pursue.

Also, a more sophisticated individual-based model, in which growth depends on food availability, turbulence, and light, in addition to transport and temperature, is needed. Among other things, this will allow us to find the optimum behaviour concerning the trade-off between feeding and favourable temperature.

### Acknowledgements

This research was performed as part of the INTEGRATION project under the German Climate Research Programme DEKLIM. The Research Council of Norway funded the co-authors through the ECOBE project. Computer time for the hydrodynamic model was granted partly by NOTUR, the super-computing programme of the Research Council of Norway. NOAA-CIRES Climate Diagnostics Center, Boulder, Colorado, USA, provided data through the NCEP/NCAR reanalysis project (<http://www.cdc.noaa.gov/>). The authors thank Karen Gjertsen (IMR) for her work on Figure 1.

### References

- Ådlandsvik, B., and Budgett, P. 2003. Adapting the Regional Ocean Model System for dynamic downscaling. RegClim General Technical Report, 7: 49–58.
- Ådlandsvik, B., and Sundby, S. 1994. Modelling the transport of cod larvae from the Lofoten area. ICES Marine Science Symposium, 198: 379–392.
- Bjørke, H., and Sundby, S. 1987. Abundance indices and distribution of postlarvae and 0-group cod. Contribution to the third Soviet-Norwegian symposium in Murmansk, 26–30 May 1986: “The effect of oceanographic conditions on distribution,

- and population dynamics of commercial fish stocks in the Barents Sea." 19 pp.
- Björnasson, B., and Steinarsson, A. 2002. The food-unlimited growth rate of Atlantic cod *Gadus morhua*. *Canadian Journal of Fisheries and Aquatic Sciences*, 59: 494–502.
- Budgell, W. P. 2005. Numerical simulation of ice-ocean variability in the Barents Sea region. *Ocean Dynamics* (in press).
- Chapman, D. C. 1985. Numerical treatment of cross-shelf open boundaries in a barotropic coastal ocean model. *Journal of Physical Oceanography*, 15: 1060–1075.
- Csanady, G. T. 1973. Turbulent diffusion in the environment. *Geophysical and Astrophysical Monographs*, vol. 3: D. Reidel, Rotterdam.
- Ellertsen, B., Fossum, P., Solemdal, P., and Sundby, S. 1989. Relation between temperature and survival of eggs and first-feeding larvae of northeast Arctic cod *Gadus morhua* L. *Rapports et Procès-Verbaux des Réunions du Conseil International pour l'Exploration de la Mer*, 191: 209–219.
- Engedahl, H., Ådlandsvik, B., and Martinsen, E. A. 1998. Production of monthly mean climatological archives of salinity, temperature, current and sea level for the Nordic Seas. *Journal of Marine Systems*, 14: 1–26.
- Fiksen, Ø., Utne, A. C. W., Aksnes, D. L., Eiane, K., Helvik, J. V., and Sundby, S. 1998. Modelling the influence of light, turbulence and ontogeny on ingestion rates in larval cod and herring. *Fisheries Oceanography*, 7: 355–363.
- Flather, R. A. 1976. A tidal model of the northwest European continental shelf. *Memories de la Societe Royale des Sciences de Liege*, 10: 141–164.
- Gallego, A., Heath, M. R., Basfred, D. J., and MacKenzie, B. R. 1999. Variability in growth rates of larval haddock in the northern North Sea. *Fisheries Oceanography*, 8: 77–92.
- Heath, M. R., and Gallego, A. 1998. Bio-physical modeling of the early life stages of haddock, *Melanogrammus aeglefinus*, in the North Sea. *Fisheries Oceanography*, 7: 10–125.
- Hinrichsen, H. H., Bottcher, U., Koster, F. W., Lehmann, A., and St. John, M. A. 2003. Modeling the influences of atmospheric forcing conditions on Baltic cod early life stages: distributions and drift. *Journal of Sea Research*, 49: 187–201.
- Hinrichsen, H. H., Mollmann, C., Voss, R., Koster, F. W., and Kornilovs, G. 2002. Biophysical modeling of larval Baltic cod (*Gadus morhua*) growth and survival. *Canadian Journal of Fisheries and Aquatic Sciences*, 59: 1858–1873.
- Hjort, J. 1914. Fluctuation in the great fisheries of northern Europe viewed in the light of biological research. *Rapports et Procès-Verbaux des Réunions du Conseil Permanent International pour l'Exploration de la Mer*, 20: 1–228.
- ICES. 1985. Preliminary report of the International 0-Group Fish Survey in the Barents Sea and Adjacent Waters in August–September 1985. *ICES CM 1985/G. 75*.
- ICES. 1986. Preliminary report of the International 0-Group Fish Survey in the Barents Sea and Adjacent Waters in August–September 1986. *ICES CM 1986/G. 78*.
- Kalnay, E., et al. 1996. The NCEP/NCAR 40-year reanalysis project. *Bulletin of the American Meteorological Society*, 77: 437–471.
- Lough, R. G., Smith, W. G., Werner, F. E., Loder, J. W., Page, F. H., Hannah, C. G., Namie, C. E., Perry, R. I., Sinclair, M., and Lynch, D. R. 1994. Influence of wind-driven advection on inter-annual variability in cod eggs and larval distributions on Georges Bank: 1982. vs. 1985. *ICES Marine Science Symposia*, 198: 356–378.
- Martinsen, E. A., and Engedahl, H. 1987. Implementation and testing of a lateral boundary scheme as an open boundary condition in a barotropic ocean model. *Coastal Engineering*, 11: 603–627.
- Mellor, G., and Yamada, T. 1982. Development of a turbulence closure model for geophysical fluid problems. *Reviews of Geophysics and Space Physics*, 20: 851–875.
- Otterlei, O., Nyhammar, G., Folkvord, A., and Stefansson, S. O. 1999. Temperature- and size-dependent growth of larval and early juvenile Atlantic cod: a comparative study of Norwegian coastal cod and northeast Arctic cod. *Canadian Journal of Fisheries and Aquatic Sciences*, 56: 2099–2111.
- Ottersen, G., and Loeng, H. 2000. Covariability in early growth and year-class strength of Barents Sea cod, haddock, and herring: the environmental link. *ICES Journal of Marine Science*, 57: 339–348.
- Ottersen, G., and Sundby, S. 1995. Effects of temperature, wind and spawning stock biomass on recruitment of Arcto-Norwegian cod. *Fisheries Oceanography*, 4: 278–292.
- Shchepetkin, A. F., and McWilliams, J. C. 2005. The regional oceanic modeling system (ROMS): a split-explicit, free-surface, topography-following-coordinate oceanic model. *Ocean Modelling*, 9: 347–404.
- Sundby, S. 1983. A one-dimensional model for the vertical distribution of pelagic fish eggs in the mixed layer. *Deep-Sea Research*, 30: 645–661.
- Sundby, S. 2000. Recruitment of Atlantic cod stocks in relation to temperature and advection of copepod populations. *Sarsia*, 85: 277–298.
- Sundby, S., Bjørke, H., Soldal, A. V., and Olsen, S. 1989. Mortality rates during the early life stages and year-class strength of northeast Arctic cod (*Gadus morhua* L.). *Rapports et Procès-Verbaux des Réunions du Conseil International pour l'Exploration de la Mer*, 191: 351–358.
- Sundby, S., and Bratland, P. 1987. Kartlegging av gytefeltene for norsk-arktisk torsk i Nord-Norge og beregning av eggproduksjonen i årene 1983–1985. *Fisken og Havet*, 1: 1–58 (In Norwegian).
- Sundby, S., and Fossum, P. 1990. Feeding conditions of Arcto-Norwegian cod larvae compared to the Rothschild-Osborn theory on small-scale turbulence and plankton contact rates. *Journal of Plankton Research*, 12: 1153–1162.
- Suthers, I. M., and Sundby, S. 1993. Dispersal and growth of pelagic juvenile Arcto-Norwegian cod, (*Gadus morhua*), inferred from otolith microstructure and water temperature. *ICES Journal of Marine Science*, 50: 261–270.
- Suthers, I. M., and Sundby, S. 1996. Role of the midnight sun: comparative growth of pelagic juvenile cod (*Gadus morhua*) from the Arcto-Norwegian and a Nova Scotian stock. *ICES Journal of Marine Science*, 53: 827–837.
- Vikebø, F. B. 2005. Impact of climate on Arcto-Norwegian cod. PhD thesis, University of Bergen.
- Voss, R., Hinrichsen, H. H., and St. John, M. 1999. Variations in the drift of larval cod (*Gadus morhua* L.) in the Baltic Sea: combining field observations and modelling. *Fisheries Oceanography*, 8: 199–211.
- Werner, F. E., Page, F. H., Lynch, D. R., Loder, J. W., Lough, R. G., Perry, R. I., Greenberg, D. A., and Sinclair, M. M. 1993. Influence of mean advection and simple behavior on the distribution of cod and haddock early life stages on Georges Bank. *Fisheries Oceanography*, 2: 43–64.
- Werner, F. E., Quinlan, J. A., Lough, R. G., and Lynch, D. R. 2001. Spatially-explicit individual based modeling of marine populations: a review of the advances in the 1990s. *Sarsia*, 86: 411–421.